Continuous Copolymerization of Vinylidene Fluoride with Hexafluoropropylene in Supercritical Carbon Dioxide: Low Hexafluoropropylene Content Semicrystalline Copolymers

Tamer S. Ahmed,[†] Joseph M. DeSimone,[†,‡] and George W. Roberts*[,†]

Department of Chemical and Biomolecular Engineering, North Carolina State University, Box # 7905, Raleigh, North Carolina 27695-7905, and Department of Chemistry, University of North Carolina at Chapel Hill, Box # 3290, Chapel Hill, North Carolina 27599-3290

Received June 19, 2007; Revised Manuscript Received October 24, 2007

ABSTRACT: The copolymerization of vinylidene fluoride with hexafluoropropylene (HFP) was carried out in supercritical carbon dioxide by precipitation polymerization using a continuous stirred tank reactor. Copolymers with ca. 10 mol % HFP were synthesized at 40 °C and pressures in the range of 207−400 bar using perfluorobutyryl peroxide as the free radical initiator. The effects of feed monomer concentration and reaction pressure were both explored at otherwise constant conditions. The rate of polymerization (R_p) and the number-average molecular weight (M_n) increased linearly with the total monomer concentration up to about 6 M, the highest concentration investigated. The R_p and the M_n were strongly influenced by the reaction pressure. An 80% increase in both R_p and M_n was observed when the reaction pressure rose from 207 to 400 bar. The molecular weight distributions of the synthesized copolymer showed a long tail that increased to become a broad shoulder with increasing total monomer concentration. This tail increased with increasing reaction pressure. The data suggest that the carbon dioxide-rich fluid phase is the primary locus of polymerization.

Introduction

Supercritical carbon dioxide ($scCO_2$) has emerged as a sustainable alternative to the aqueous and organic media often used in polymer processes.[1−6] Supercritical carbon dioxide has unique properties including being environmentally benign, nontoxic, nonflammable, and inexpensive. Using $scCO_2$ as a polymerization medium allows additional benefits, including inertness to free radicals[7] which eliminates chain transfer to solvent and high initiator efficiencies[7−9] as a result of its low viscosity.

From an industrial perspective, $scCO_2$-based polymerization processes have many advantages over aqueous suspension and emulsion polymerization processes. First, the elimination of water and organic solvents results in the reduction of undesirable effluents from the processes. Second, the production of the polymer directly in a dry form potentially eliminates many separation steps and reduces the extensive energy consumption associated with drying. Third, it may be possible to polymerize monomers that are difficult or even impossible to be used in an aqueous system, either because of their solubility or because of their reaction with water. Fourth, the polymers produced may have some distinct physical or structural properties, which may facilitate processing or open new applications for such polymers.[10,11] Finally, the use of perfluorooctanoic acid (PFOA), also known as "C8", is eliminated. C8 is a perfluorinated anionic surfactant used as a dispersing agent in the water-based polymerization and copolymerization of many fluoropolymers.[12] In 2003, the United States Environmental Protection Agency (EPA) released a preliminary risk assessment of C8.[12] In January 2006, the EPA initiated a program to reduce PFOA releases and its presence in products by 95% by no later than 2010 and to work toward eliminating these sources of exposure no later than 2015.[13] To date, no viable, alternative dispersing agent has been publicly identified. Polymerization in $scCO_2$ is the only known alternative that can eliminate the need for C8 in the manufacturing process.[6]

A continuous process is essential to harness the advantages of using $scCO_2$ as a polymerization medium for high-volume polymers. Relative to batch polymerization, continuous processing requires smaller equipment per unit of throughput and therefore is less capital intensive. This is a particular advantage for processes involving $scCO_2$ because relatively high pressures are intrinsic. In addition, continuous polymerization leads to a more uniform product because of the time-invariant reaction conditions and to easier recycle of unreacted monomer and CO_2. Moreover, continuous operation offers the potential to couple polymerization with continuous downstream processing. Finally, the startup of a commercial facility to produce various grades of Teflon in $scCO_2$ by continuous polymerization underscores the potential industrial importance of the CO_2-based continuous polymerization technology.[14,15]

Vinylidene fluoride-based copolymers, typically called PVDF copolymers, have become the products of choice in many applications.[16] Copolymers of vinylidene fluoride (VF2) with hexafluoropropylene (HFP) are one of the most important PVDF copolymers.[17] Low HFP content copolymers, also known as "flexible PVDF", are thermoplastic and semicrystalline copolymers containing about 5−15 mol % HFP.[18,19] They are used in many applications including tubing, valves and fittings, cable and wire jacketing, lithium ion batteries, and membranes. When the HFP content is higher than 19−20 mol %, the copolymers are amorphous and elastomeric.[20,21] The maximum theoretical incorporation of HFP in the copolymer is restricted only to 50 mol % because of the reactivity ratio of HFP.[22−24] Most commercial poly(VF2-*co*-HFP) elastomers contain around 22 mol % HFP,[25] a composition that represents the best compromise between a low glass transition temperature (T_g) and a fully

* To whom correspondence should be addressed: Tel +1-919-515−7328; Fax +1-919-515-3465; e-mail groberts@eos.ncsu.edu.
[†] North Carolina State University.
[‡] University of North Carolina at Chapel Hill.

10.1021/ma0713613 CCC: $37.00
Published on Web 11/30/2007

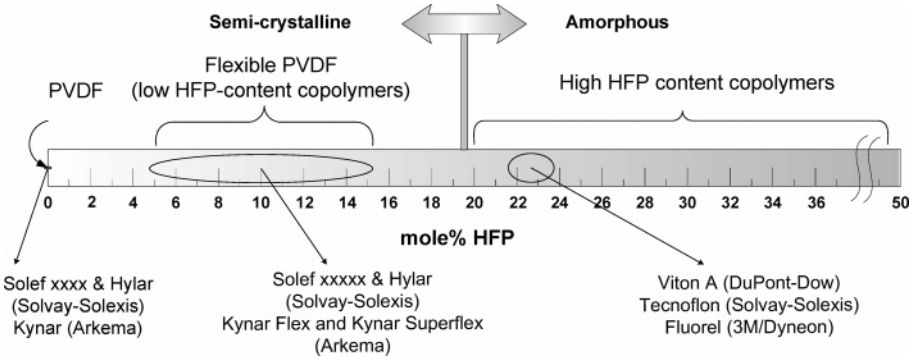

Figure 1. Different copolymers of VF2 with HFP with their main manufacturers and trade names.

amorphous polymer. The high HFP content copolymers are used mainly as polymer processing aids to improve extrusion, blow molding, and rotomolding and in sealing such as in gaskets and O-rings. Figure 1 shows different poly(VF2-*co*-HFP) copolymers with their main manufacturers and trade names.

Low HFP content copolymers are typically manufactured commercially by aqueous emulsion or suspension polymerization.[26,27] Only aqueous emulsion techniques are used for the high HFP content copolymers[20,28−30] because of their tacky nature.[31] Both processes generate a large quantity of wastewater and require a substantial quantity of energy for drying the polymer product, if drying is required.[32] As a result of the ionic end groups from the initiator (ammonium or potassium persulfate or the redox persulfate/sodium sulfite system[30]), PVDF copolymers tend to be self-emulsified for low solids content polymerizations.[33] However, for high solids content processes, PFOA salts are used.[34] Polymerization in $scCO_2$ offers a "green" solution to the above problems and challenges.

Our research group has reported a process for the continuous precipitation polymerization of chain-growth polymers in $scCO_2$ using a continuous stirred-tank reactor (CSTR).[35] This process has been applied for the continuous precipitation polymerization of both poly(vinylidene fluoride) (PVDF)[9,35−37] and poly(acrylic acid) (PAA).[10,38,39] Here, we report the continuous precipitation copolymerization of low HFP content copolymers in $scCO_2$ using a modified version of the above-mentioned continuous process. To date, copolymerization of VF2 with HFP in $scCO_2$ has been reported only in batch reactors.[40−42] This paper will underline the advantages of $scCO_2$ as a polymerization medium. In addition, it is the first report of any continuous copolymerization in $scCO_2$.

Experimental Section

Materials. Carbon dioxide (SFC grade, 99.998%, maximum O_2 = 2 ppm), nitrogen (99.999%), and argon (99.9999%) were obtained from National Specialty Gases. To completely remove O_2 from the CO_2, three Alltech High Pressure Oxy-Trap traps were installed in parallel between the CO_2 tanks and CO_2 pump. Both VF2 (99% minimum, balance N_2) and HFP (99% minimum, balance N_2) were obtained from SynQuest Laboratories. An Alltech High Pressure Oxy-Trap trap was installed between each monomer cylinder and its corresponding pump. All other chemicals were obtained from Fisher Scientific and used as received.

Initiator Synthesis. Perfluorobutyryl peroxide ($[C_3F_7COO]_2$, PBP) was the initiator used in the copolymerization. The initiator was synthesized in 1,1,2-trichloro-1,2,2-trifluoroethane (HPLC-grade, 99.8%, Freon 113), as previously reported.[43] All manipulations of the initiator were performed in a NaCl/ice bath, and the final product was stored under dry ice. The iodine titration technique, ASTM Method E 298-91, was utilized to determine the concentration of the initiator in the solution. The initiator concentration was reduced to 0.03 M by dilution with additional Freon 113 before use. After a second titration, the initiator solution was introduced to the initiator pump under an argon blanket. The half-life of PBP in Freon 113 is about 35 min at 40 °C.[43]

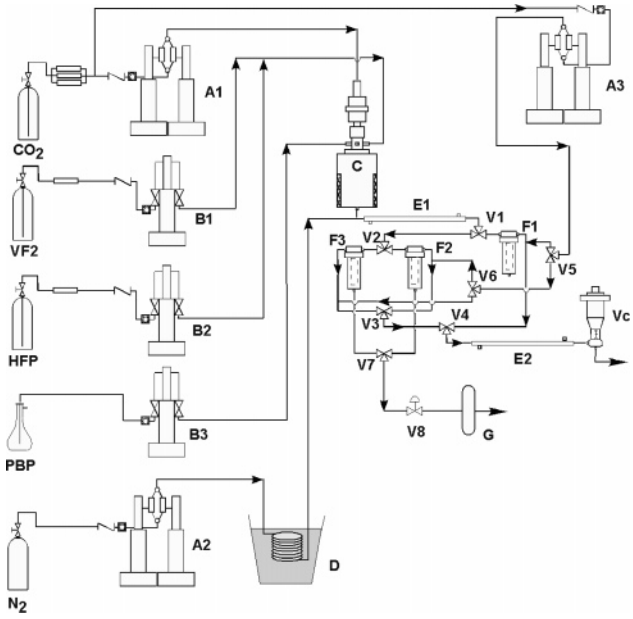

Figure 2. CSTR polymerization system. A1, A2, A3: continuous syringe pumps; B1, B2, B3: syringe pumps; C: autoclave with stirrer; D: dry ice/acetone bath; E1, E2: heat exchangers; F1: steady-state filter; F2, F3: non-steady-state filters; G: bag filter; V1, V2, V3, V4, V5, V6, V7: three-way valves; V8: two-way valve; Vc: control valve.

Polymerization Apparatus and Procedure. Figure 2 shows a schematic of the continuous polymerization system. There are some differences between the current system and the one reported previously by us for the continuous polymerization of PVDF[9,35−37] and PAA.[10,38,39] The reactor (C) is a 100 mL high-pressure autoclave (Autoclave Engineers) with a magnetically driven agitator (Autoclave Engineers). Three downward-pumping impellers were mounted on the shaft of the agitator. The current autoclave has the same length-to-diameter ratio as our previously reported 800 mL reactor used for PVDF[9,35−37] and PAA.[10,38,39] The smaller reactor allowed more flexibility in the range of reaction parameters that could be reached. In addition, a continuous syringe pump (A2, 260D Isco dual-cylinder syringe pump) was used to inject nitrogen into the effluent from the reactor (C). The nitrogen was cooled in a dry ice/acetone bath before it was injected. The role of nitrogen was (1) to increase the flow rate after the reactor to prevent settling of the effluent copolymer particles in the lines, (2) to minimize the solubility of low-molecular-weight or high-HFP polymeric chains in the effluent mixture, thereby ensuring that all the synthesized copolymer was collected in the high-pressure filters (F1, F2, F3), and (3) to quench the reaction, dilute the effluent mixture, and decrease the residence time in the filters to minimize postpolymer-

Table 1. Effect of Inlet Total Monomer Concentration on the Continuous Copolymerization of VF2 with HFP in $scCO_2$[a]

no.	$[M_T]_{in}$ (mol/L)	$[F_{HFP}]_{F-EA}$ (mol %)[b]	$[F_{HFP}]_{NMR}$ (mol %)[c]	$(R_P)_{av}$ (10^{-2} mol/(L min))[d]	$[M_T]_{out-av}$ (mol/L)[e]	X (%)[f]	$(M_n)_{NMR}$ (kDa)[g]	$(M_n)_{GPC}$ (kDa)	PDI
1	1.96	10.74	8.75	0.83	1.80	8.16	19.0	19.7	1.5
2	2.61	10.65	8.60	1.34	2.34	10.34	29.8	31.1	1.7
3	3.92	9.97	8.42	1.94	3.53	9.95	43.4	43.8	3.2
4	5.23	9.77	8.13	2.38	4.76	8.99	60.2	56.8	3.6
5	6.53	9.55	7.73	3.04	5.92	9.34	87.0	79.2	3.9

[a] Reaction conditions: $P = 400$ bar; $T = 40$ °C; $\tau = 20$ min; $[I]_{in} = 0.003$ M; HFP/VF2 molar feed ratio = 26.5/73.5. [b] HFP incorporation in the copolymer from fluorine elemental analysis (eq 3). [c] HFP incorporation in the copolymer from NMR (eq 4). [d] Average molar rate of polymerization based on the average of $[F_{HFP}]_{F-EA}$ and $[F_{HFP}]_{NMR}$ (eq 1). [e] Average total monomer concentration inside the reactor and in the effluent based on the average of $[F_{HFP}]_{F-EA}$ and $[F_{HFP}]_{NMR}$ (eq 2). [f] Total conversion. [g] Number-average molecular weight calculated from initiator end-group analysis by NMR (eq 5).

Table 2. Effect of Reaction Pressure on the Continuous Copolymerization of VF2 with HFP in $scCO_2$[a]

no.	P (bar)	$[F_{HFP}]_{F-EA}$ (mol %)	$[F_{HFP}]_{NMR}$ (mol %)	$(R_P)_{av}$ (10^{-2} mol/(L min))	$[M_T]_{out-av}$ (mol/L)	X (%)	$(M_n)_{NMR}$ (kDa)	$(M_n)_{GPC}$ (kDa)	PDI
4	400	9.77	8.13	2.38	4.76	8.99	60.2	56.8	3.6
6	310	9.76	8.50	1.94	4.84	7.46	37.8	43.1	2.5
7	207	10.6	8.71	1.34	4.96	5.16	28.5	31.8	1.7

[a] Reaction conditions: $[M_T]_{in} = 5.23$ mol/L; $T = 40$ °C; $\tau = 20$ min; $[I]_{in} = 0.003$ M; HFP/VF2 molar feed ratio = 26.5/73.5.

ization. This was especially important since PBP is a very active initiator.[43] In addition, two heat exchangers were used: one at the reactor exit (E1) and one after the filters (E2). A cold refrigerant (−10 °C) was used in these heat exchangers to stop the initiator decomposition and minimize postpolymerization.

In a typical experiment for copolymerization of VF2 and HFP, the reactor (C) and the high-pressure filters (F1, F2, F3) were purged three times with CO_2 at 1500 psig to remove oxygen. Syringe pumps A1, A2, B1 (cooled by 15 °C refrigerant), B2 (cooled by 15 °C refrigerant), and B3 (cooled by −7.5 °C refrigerant) were used to feed CO_2, N_2, VF2, HFP, and PBP solution in Freon 113, respectively. The speed of the reactor agitator was fixed to 2000 rpm in all the runs. The outlet stream from the reactor, consisting of the copolymer particles, CO_2, and unreacted VF2, HFP, and PBP, plus the nitrogen that was injected into the effluent from the reactor, was directed by a three-way ball valve (V1) either into the steady-state filter housing (F1) or to another three-way ball valve (V2) to direct the stream to the unsteady-state filters (F2 and F3). All filters contained 1 μm stainless steel mesh filter media. During startup of the reactor, before steady state was attained, the copolymer was collected in one of the unsteady-state filters (e.g., F2) until it was filled (indicated by the pressure drop across the filter). Valves V2 and V3 then were switched, so that the copolymer was being collected in the other unsteady-state filter (F3). The particles then were discharged from filter F2 by back-flushing with a CO_2 stream from a continuous syringe pump (A3). Valves V7 and V8 then were actuated sequentially, with V7 being closed before V8 was opened, allowing the copolymer particles to flow from the high-pressure filter housing into the bag filter, which was at ambient pressure. When filter F3 was nearly full, the stream leaving the reactor was switched back to filter F2, and filter F3 was emptied using the same technique. This procedure was repeated until the reactor had reached steady state after five average residence times. The stream leaving the reactor then was switched to the steady-state filter (F1) using valves V1 and V4. The copolymer particles were collected for at least one residence time. The system was then shut down, and the residual monomers and initiator were extracted three times from the copolymer using CO_2 from the continuous syringe pump A3. Finally, the filter F1 was opened and the copolymer was collected and weighed. In all the experiments, a homopolymerization of VF2 was first carried out in the reactor, followed by flushing the reactor with CO_2. This was followed by baking the PVDF layer at 100 °C for 30 min before starting the copolymerization of VF2 and HFP. Finally, the monomer densities that were used to calculate the flow rates out of the pump were corrected for pressure using the Hakinson−Brobst−Thomson method.[44,45]

Characterization. Gel permeation chromatography (GPC) was performed at 40 °C using a Waters 150-CV GPC equipped with Waters Styragel HR 5, 4, 2, and 0.5 columns and a refractive index detector. Tetrahydrofuran was used as the mobile phase, and polystyrene standards were used for the calibration.

Hydrogen, carbon, and fluorine elemental analysis were performed by Atlantic Microlab, Inc. Hydrogen and carbon analyses were performed by combustion using automatic analyzers while fluorine analyses was performed by flask combustion followed by ion chromatography.

Fluorine-19 nuclear magnetic resonance (^{19}F NMR) spectra were recorded on a Bruker Avance spectrometer operating at 470.6 MHz using acetone-d_6 (99.9%) as the solvent and trichlorofluoroethane ($CFCl_3$) as the internal reference. Pulse delay was 5 s, and 256−1024 scans were used.

Differential scanning calorimetry (DSC) measurements were conducted using a TA Instruments DSC-Q100. The instrument was calibrated using indium. Samples were heated to 200 °C at a heating rate of 10 °C/min. The glass transition temperature, the melting temperature, and the heat of melting were determined from the second heating curve.

Finally, a thermal gravimetric analyzer (TA Instruments TGA-Q500) was used for determining the decomposition temperature (T_d) of the synthesized copolymers. Samples were heated to 850 °C at a heating rate of 10 °C/min in nitrogen atmosphere. The T_d was determined for 1 wt % polymer loss.

Results and Discussion

Copolymerization Studies. Experiments were carried out to study the effect of total inlet monomer concentration ($[M_T]_{in}$) and reaction pressure (P) on the copolymerization of VF2 with HFP at 40 °C in the CSTR using PBP initiator. The results of these experiments are shown in Tables 1 and 2, respectively. The copolymers were characterized for their composition, average molecular weight, and molecular weight distribution (MWD). The molar rate of polymerization (R_P) and the total monomer concentration in the reactor and in the outlet stream ($[M_T]_{out}$) were calculated from the amount of polymer collected (m_p) during the time of steady-state collection (Δt_{ss}) using eqs 1 and 2, respectively. Equations 1 and 2 are based on the assumption that the reactor behaved as an ideal CSTR.

$$R_p = \frac{m_p}{V_R \Delta t_{ss}([F_{HFP}]M_{HFP} + (1 - [F_{HFP}])M_{VF2})} \quad (1)$$

$$[M_T]_{out} = [M_T]_{in} - R_P\tau \quad (2)$$

where V_R is the reactor volume (100 mL), $[F_{HFP}]$ is the mole fraction of HFP in the copolymer, M_{HFP} and M_{VF2} are the molecular weights of HFP and VF2, respectively, and τ is the average residence time in the reactor.

The copolymer composition was determined by both fluorine elemental analysis and ^{19}F NMR. All elemental analyses were determined on a weight basis with accuracy and precision error limits of ±0.3 wt %. The error of the elemental analyses on a mole basis depends on the molecular weight of the analyzed element. Since fluorine has the highest molecular weight of the three elements forming the copolymer (hydrogen, carbon, and fluorine), only fluorine elemental analysis (F-EA) was considered. For 10 mol % HFP poly(VF2-*co*-HFP), the ±0.3 wt % error limit corresponds to about ±1 mol% HFP. Equation 3 was used to calculate $[F_{HFP}]_{F-EA}$ (mole fraction HFP in the copolymer from F-EA) from the average of two measurements $(W_F)_{av}$ (average weight fraction of fluorine in the copolymer).

$$[F_{HFP}]_{F-EA} = \frac{19 - 32(W_F)_{av}}{43(W_F)_{av} - 38} \quad (3)$$

A representative ^{19}F NMR spectrum for poly(VF2-*co*-HFP) is given in Figure 3. The detailed chemical shifts are available in the literature.[23,46] The ^{19}F NMR spectrum exhibits various groups of signals; those assigned to VF2 units are centered at −91.4 to −96.2 ppm for head-to-tail normal additions (−$CH_2C\mathbf{F}_2$-CH_2CF_2−), at −108.6 to −112.3 ppm for CF_2 groups adjacent to a HFP unit (−$CH_2C\mathbf{F}_2CF_2CF(CF_3)$−), and at −113.6 and −115.9 ppm for the head-to-head reversed addition (−$CH_2C\mathbf{F}_2$-CF_2CH_2−). Those assigned to HFP units are centered at −70.3 and −75 ppm for the pendant CF_3 group (−$CF_2CF(C\mathbf{F}_3)$−), at −115.3 and −117 to −119.2 ppm for CF_2 (−$C\mathbf{F}_2CF(CF_3)$−) group, and at −181.4 and −184.1 ppm for the CF (−$CF_2C\mathbf{F}(CF_3)$−) group. Finally, the peaks at ca. −80 ppm and −126 to −127 ppm are assigned to the $-CF_3$ and $-CF_2$ fluorine in the initiator, respectively.

The mole fraction of HFP monomer in the copolymer ($[F_{HFP}]_{NMR}$) was calculated from eq 4

$$[F_{HFP}]_{NMR} = \frac{B}{A + B} \quad (4)$$

where *A* corresponds to the sum of the areas of the NMR signals from −91.4 to −115.9 ppm and *B* corresponds to the sum of the areas of the NMR signals from −117 to −119.2 ppm (Figure 3). The copolymer composition obtained via fluorine elemental analysis was always higher than that from NMR. Nevertheless, the two compositions are close enough to lend confidence to the results.

In addition, NMR was used to determine the number-average molecular weight (M_n) from end-group analysis of the initiator. Usually, end-group analysis is accurate only for M_n below 20−30 kDa.[47] However, this rule of thumb is primarily applied to hydrocarbon polymers. For fluorinated polymers, since fluorine has a much higher molecular weight than hydrogen, the average molecular weight of the repeating unit in the polymer is higher than for hydrocarbon polymers. Consequently, for the same degree of polymerization, end-group analysis can be used to determine M_n to higher values for fluorinated polymers than for hydrocarbon polymers. The number-average molecular weight using the end-group analysis of the PBP initiator by NMR ($(M_n)_{NMR}$) was calculated via eq 5.

$$(M_n)_{NMR} = \frac{(I_{CF_2})/2}{(I_{-80\ ppm}/3)/2}[150[F_{HFP}]_{NMR} + 64(1 - [F_{HFP}]_{NMR})] \quad (5)$$

Here, $I_{-80\ ppm}$ is the integral of the signal corresponding to the fluorine of the CF_3 group in the C_3F_7 of the PBP initiator located at ca. −80 ppm; I_{CF_2} is the sum of the integrals for the signals corresponding to the fluorine in CF_2 groups in the copolymer from −91.4 to −119.2 ppm (A + B in Figure 3).

The main assumption in eq 5 is that termination is by combination. This accounts for the factor of 1/2 that multiplies ($I_{-80\ ppm}/3$) in the denominator. This assumption is consistent with PDI values around 1.5 observed previously for the homopolymerization of VF2 in CO_2,[37] for the batch copolymerization of VF2 and HFP,[40] and in this work for low feed monomer concentrations (e.g., experiments 1 and 2 in Table 1). Another assumption is that chain transfer reactions to monomer and initiator are unimportant. There is no evidence from the literature that chain transfer to VF2 can occur, while chain transfer to HFP, PBP, or Freon 113 is unlikely since they do not contain hydrogen.

Molecular weights were assessed using both GPC and NMR end-group analysis. Both agree reasonably well for low molecular weights. For the high molecular weights, small deviations appear between the molecular weights from GPC and NMR end-group analysis (Table 1). The agreement between the two techniques may be somewhat fortuitous since the GPC results are relative to polystyrene standards and in view of the assumptions in the NMR end-group calculation.

Morphology. Figure 4 shows scanning electron micrographs (SEM) for VF2-HFP copolymer collected in experiment 4 at 40 °C. The particles generally show spherulitic structures with diameters ∼10−50 μm. In addition, they show a relatively porous structure that would offer little resistance to transport of small molecules such as monomers or initiator.

Thermal Properties. Table 3 shows the thermal properties for the highest molecular weight copolymer synthesized in this work (experiment 5, Table 1). As expected, the introduction of the $-CF_3$ side group arising from HFP into the backbone of the copolymer raised the glass transition temperature (T_g) compared to PVDF homopolymer (typical T_g for PVDF = −40 °C[48]).

Effect of Total Monomer Concentration. Five experiments were carried out with $[M_T]_{in}$ varying from 1.96 to 6.53 mol/L at otherwise identical conditions. The results are given in Table 1 and Figure 5a−d. In a CSTR, the concentration that affects the polymerization is the concentration inside the reactor, which is the same as the effluent concentration ($[M_T]_{out}$). Consequently, the results in Figure 5 are plotted vs the average $[M_T]_{out}$ from F-EA and NMR. All experiments were run with the same temperature, average residence time (τ), and feed initiator concentration ($[I]_{in}$). Therefore, the initiator concentration in CSTR and in the effluent ($[I]_{out}$) should be the same for each of these experiments (eq 6).

$$[I]_{out} = \frac{[I]_{in}}{1 + k_d\tau} \quad (6)$$

where k_d is decomposition rate constant of the initiator.

Parts a and b of Figure 5 show the effect of $[M_T]_{out}$ on R_P and $(M_n)_{GPC}$, respectively. In both figures, the increase in $[M_T]_{out}$ results in a linear increase in both R_P and $(M_n)_{GPC}$. The dotted lines in Figure 5a,b represent the best fit of the experimental data by a straight line passing through the origin. The coefficient

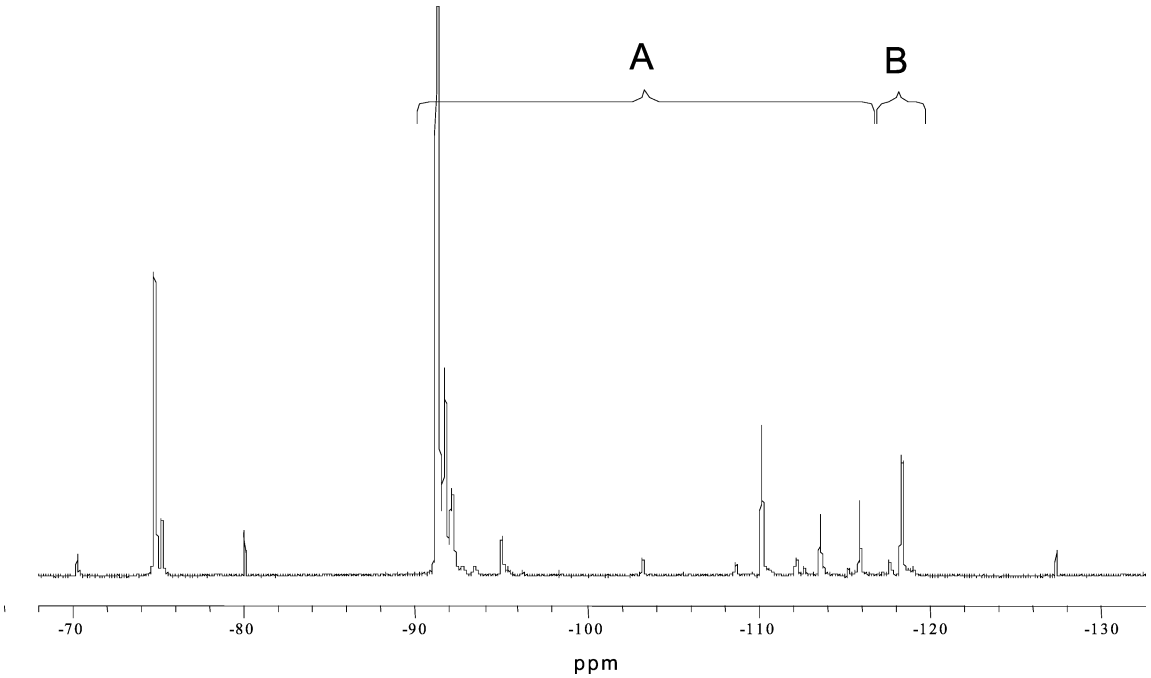

Figure 3. ^{19}F NMR spectrum for 10 mol % HFP poly(VF2-*co*-HFP) collected in experiment 3 in Table 1. The resonances due to the CF fluorine in HFP at ca. −181 to −184 ppm are not shown. Copolymer compositions were determined by the integrals of the peaks in the A and B regions.

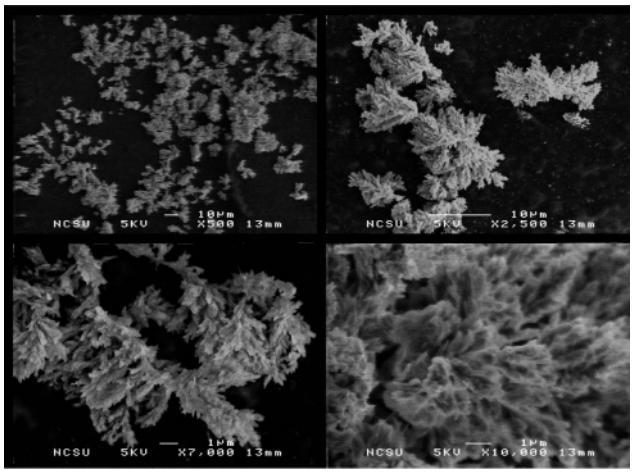

Figure 4. SEM images of VF2−HFP copolymer collected in experiment 4 in Table 1. Images are with increasing magnification.

Table 3. Thermal Properties of Poly(VF2-*co*-HFP) Synthesized in Experiment 5 in Table 1

	T_g[a] (°C)	T_m[b] (°C)	ΔH_m[c] (J/g)	T_d[d] (°C)
experiment 5	−31.4	120.7	16.5	418.1

[a] Glass transition temperature. [b] Melt peak temperature. [c] Heat of melting. [d] 1 wt % decomposition temperature in nitrogen.

of determination (R^2) of the fit is near unity in both figures. The first-order dependence of R_P and M_n on the monomer concentration is characteristic of a conventional solution polymerization. This behavior is different from what was reported in the case of the precipitation polymerization of PAA in $scCO_2$, where the order of the polymerization with respect to $[M_T]_{out}$ was significantly greater than unity for both R_P and the viscosity-average molecular weight.[38]

Parts b (right *y*-axis) and c of Figure 5 show the polydispersity indices (PDI) and the corresponding molecular weight distributions (MWDs) of the synthesized copolymers, respectively. The increase in $[M_T]_{out}$ resulted in major changes in the shape of the MWDs. For low $[M_T]_{out}$, the distribution is perfectly unimodal with a PDI of 1.5. As $[M_T]_{out}$ increases, a long tail develops and increases into a broad shoulder for the highest monomer concentration. This behavior is similar to what was observed in the precipitation polymerization of VF2 in $scCO_2$.[37] However, the MWDs of PVDF homopolymer showed distinct bimodal MWDs and higher PDIs at lower monomer concentrations.

Finally, Figure 5d shows the effect of total monomer concentration on HFP incorporation into the copolymer. Both fluorine elemental analysis and NMR show a slight decrease in HFP incorporation with increasing total monomer concentration. Since the rate of polymerization increases with total monomer concentration (Figure 5a), the copolymer volume fraction in the CSTR also increases. The decrease in HFP may be connected to this increase in the copolymer solid content in the CSTR.

Effect of Reaction Pressure. The effect of pressure was evaluated from 207 to 400 bar at otherwise identical conditions. The results are given in Table 2 and Figure 6a−d. The effect of pressure on the monomer densities was taken into account, ensuring that only pressure was affecting the polymerization.

Figure 6a,b shows that the reaction pressure has a significant effect on both R_P and $(M_n)_{GPC}$. Doubling the pressure results in about an 80% increase in both R_P and $(M_n)_{GPC}$. From transition-state theory, the effect of pressure on a rate constant can be assessed from eq 7. Assuming that the activation volume is constant over the pressure range under consideration, eq 7 can be integrated to give eq 8.

$$\frac{\mathrm{d}\ln k}{\mathrm{d}P} = -\frac{\Delta V^*}{RT} \tag{7}$$

$$k_2 = k_1 \exp\left(-\frac{\Delta V^*}{RT}(P_2 - P_1)\right) \tag{8}$$

where ΔV^* is the activation volume, R is the universal gas constant, T is the temperature, and k_1 and k_2 are the rate constants at pressures P_1 and P_2, respectively.

For typical values of the overall activation volume of polymerization (−0.01 to −0.03 L/mol),[49] the maximum

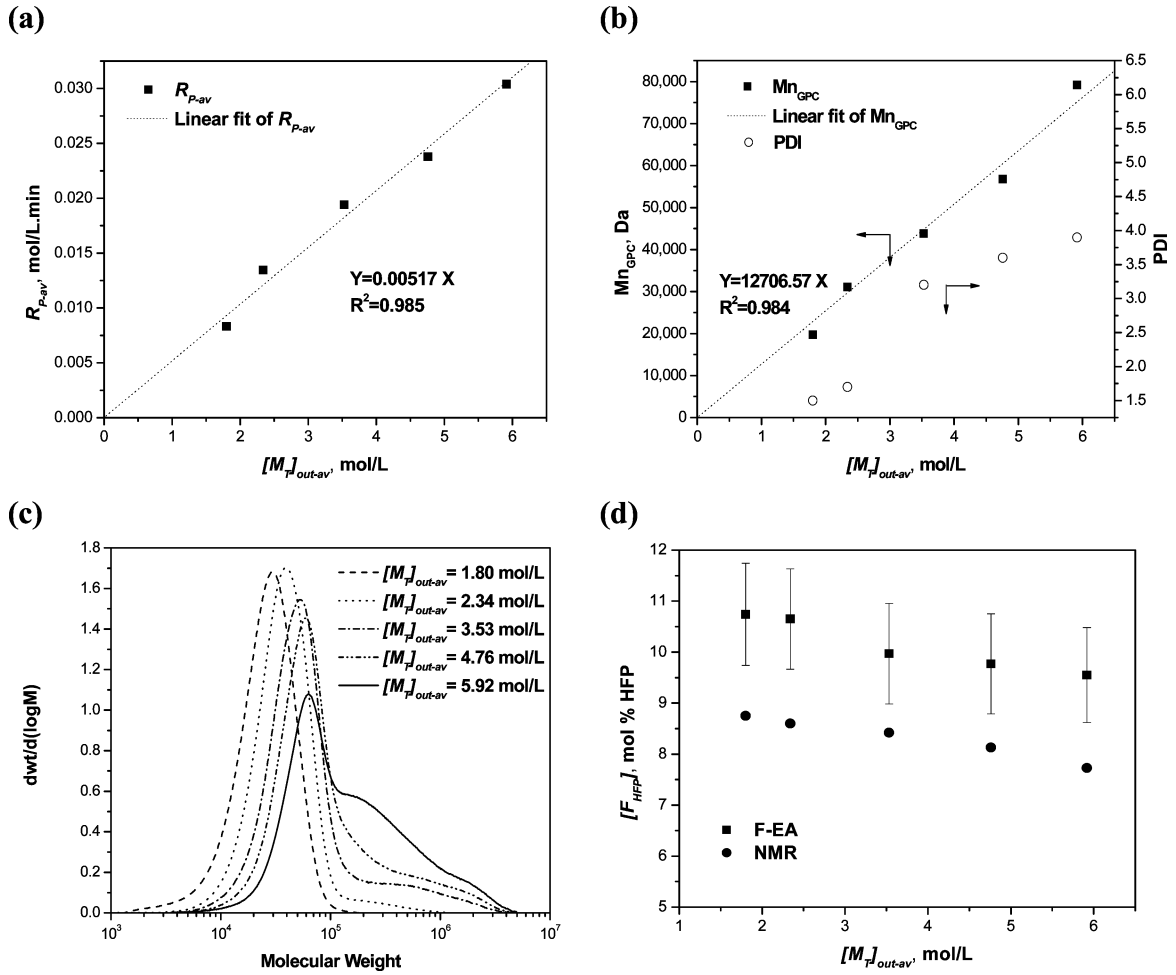

Figure 5. Effect of total monomer concentration on (a) R_P, (b) M_n and PDI, (c) MWDs, and (d) $[F_{HFP}]$. Reaction conditions are in Table 1.

increase in the apparent rate constant of polymerization for the pressure range 207−400 bar is calculated to be only about 25%. Therefore, the observed effect of pressure cannot be explained completely only by the effect of pressure on the reaction rate constants. This issue of pressure dependence is revisited in the final portion of this section.

Parts b (right *y*-axis) and c of Figure 6 show the effect of pressure on the PDI and the corresponding MWDs of the synthesized copolymers, respectively. Pressure impacts both the PDI and the MWD significantly. The increase of pressure from 207 to 400 bar results in an increase in the PDI from 1.7 to 3.6, caused by the increase in the tail of the MWD with pressure.

Finally, Figure 6d shows the effect of the pressure on HFP incorporation into the copolymer. Similar to the effect of total monomer concentration, HFP in the copolymer decreases slightly with the increase of pressure and with the increase in the amount of copolymer in the reactor. However, this decrease is within the error of the analysis.

Copolymerization Reaction Constants. Equations 9 and 10 describe the rate of polymerization and the number-average molecular weight, respectively, for a classical solution polymerization. For a copolymerization at constant temperature and pressure, the copolymerization propagation rate constant (k_p) is a function of the mole fractions of the monomers and their reactivity ratios. Equation 11 shows the expression for k_p in the case of the terminal model.[47] The termination rate is usually diffusion controlled.[47,50] For a copolymerization, the simplest "ideal diffusion" model for the copolymerization rate constant (k_t) is given by a linear combination of the termination rate constants for the two homopolymerizations (eq 12).[51]

$$R_p = k_p\left(\frac{2fk_d}{k_t}\right)^{0.5}[M][I]^{0.5} \tag{9}$$

$$M_n = \alpha M_0 k_p (2fk_d k_t)^{-0.5}[M][I]^{-0.5} \tag{10}$$

$$\bar{k}_p = \frac{r_1 f_1^2 + 2f_1 f_2 + r_2 f_2^2}{(r_1 f_1/k_{11}) + (r_2 f_2/k_{22})} \tag{11}$$

$$k_t = F_1 k_{t1} + F_2 k_{t2} \tag{12}$$

where f is the initiator decomposition efficiency; [M] and [I] are the concentrations of monomer(s) and initiator in the reactor; f_i, F_i, r_i, k_{ii}, and k_{ti} are the mole fraction in the feed, mole fraction in the copolymer, reactivity ratio, self-propagation (homopropagation) rate constant, and self-termination (homotermination) rate constant for monomer i, respectively; α equals 1 or 2 for termination by disproportionation or combination respectively; and M_0 is the average molecular weight of a monomer unit in the polymer.

Setting $[M] = [M_T]_{out}$ and $[I] = [I]_{out}$ in eqs 9 and 10, and combining them with eq 6, shows that R_p and M_n should be linear functions of $[M_T]_{out}$. This is the behavior shown by the experimental data presented in Figure 5a,b. By fitting the data to eqs 9 and 10, values of $k_p/k_t^{0.5}$ for the copolymerization of VF2 with HFP and k_d for PBP decomposition in $scCO_2$ at 40 °C and 400 bar can be estimated. Since there is no evidence in

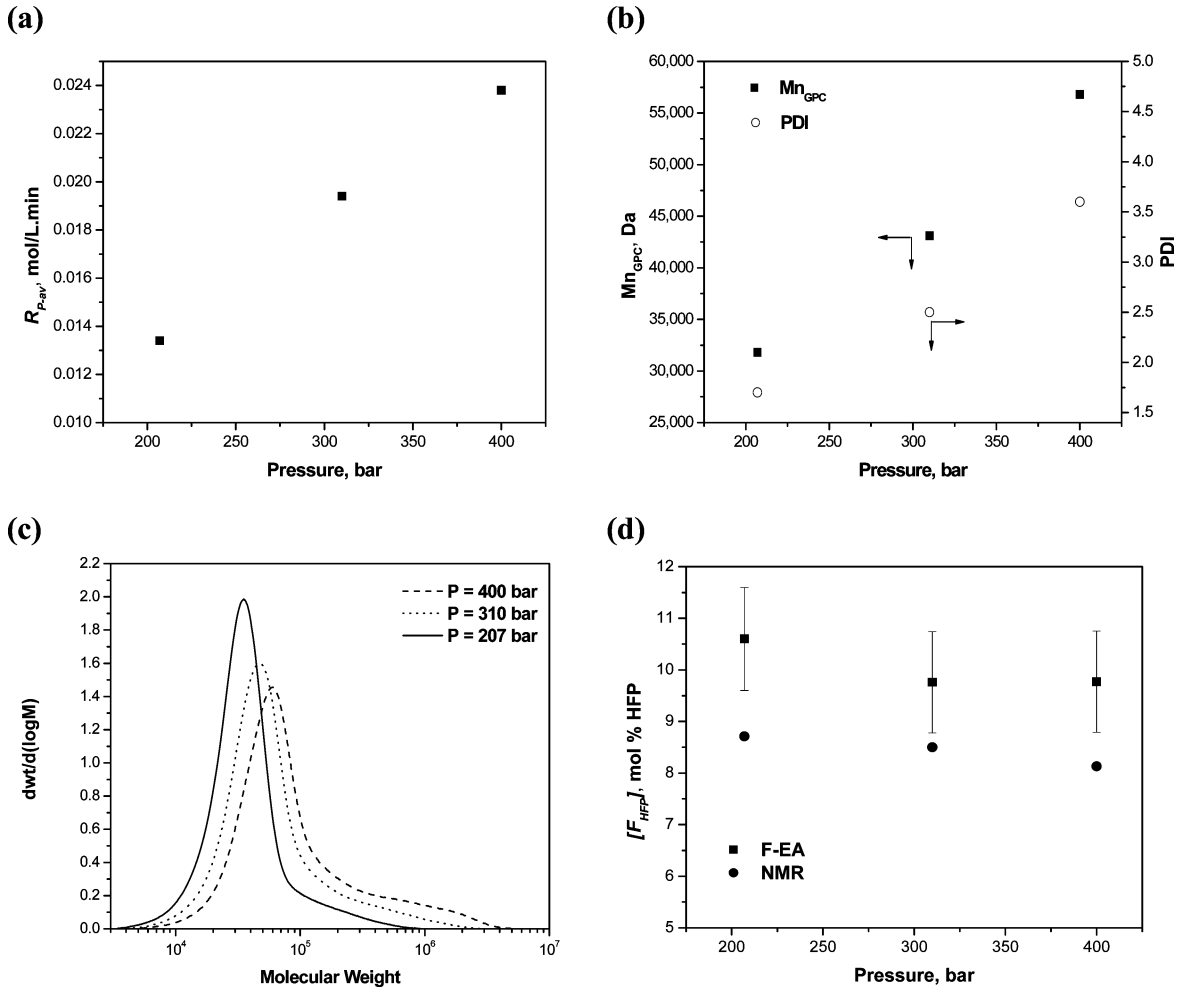

Figure 6. Effect of reaction pressure on: (a) R_P, (b) M_n and PDI, (c) MWDs, and (d) $[F_{HFP}]$. Reaction conditions are in Table 2.

Table 4. Continuous Homopolymerizations of VF2 in $scCO_2$ Using PBP Initiator[a]

$[M_T]_{in}$ (mol/L)	R_P (10^{-2} mol/(L min))	$[M_T]_{out}$ (mol/L)
1.97	1.52	1.66
2.62	1.95	2.23

[a] Reaction conditions: $P = 276$ bar; $T = 40$ °C; $\tau = 20$ min; $[I]_{in} = 0.003$ M.

the literature for termination by disproportionation,[37] termination by combination was assumed and a value of $\alpha = 2$ was used. A value of $f = 0.6$ was assumed, similar to that observed for diethyl peroxydicarbonate decomposition in $scCO_2$.[9] A value of $M_0 = 71.94$ was calculated from the average of the values of the copolymer compositions from F-EA and NMR (Table 1). Only molecular weight data from GPC were used, although they are against polystyrene standards. However, as shown in Tables 1 and 2, the differences between molecular weights from GPC and NMR end-group analysis are small.

It is interesting to compare the values of $k_p/k_t^{0.5}$ for the copolymerization of VF2 with HFP with those of the homopolymerization of VF2 in $scCO_2$. Unfortunately, the values of $k_p/k_t^{0.5}$ for VF2 homopolymerization that are available in the literature were obtained at completely different conditions with a different initiator.[36] To obtain an approximate value for comparison at the same conditions, two homopolymerizations of VF2 were carried out at 276 bar and 40 °C using PBP initiator. The results are shown in Table 4. Since there is not much effect of pressure on the rate of initiator decomposition in CO_2,[8,9] the value of k_d calculated from the copolymer data

Table 5. Values for $k_p/k_t^{0.5}$ for Poly(VF2-*co*-HFP) and PVDF and k_d of the PBP Initiator ($P = 400$ bar and $T = 40$ °C)

	$k_p/k_t^{0.5}$ ($L^{0.5}/(mol^{0.5}\ s^{0.5})$)	k_d ($10^{-4}\ s^{-1}$)
poly(VF2-*co*-9.2 mol % HFP)	0.68	4.01
PVDF	1.3	-

was used in eq 9. For the homopolymer, eq 8 was used to adjust the value of $k_p/k_t^{0.5}$ to 400 bar. The activation volume for $k_p/k_t^{0.5}$ ($\Delta V^*_p - {}^1/_2\Delta V^*_t$) was estimated from eq 13 using an overall polymerization activation volume (ΔV^*_{poly}) of -0.025 L/mol.[49] Since solvent cage effects are minimal in the case of CO_2,[8] the activation volume for the initiator decomposition (ΔV^*_d) was taken to be $+0.0045$ L/mol.[47] A calculation based on eq 8 then shows that $k_p/k_t^{0.5}$ of PVDF homopolymer increases by about 14% from 276 to 400 bar.

$$\Delta V^*_{poly} = \Delta V^*_p - \frac{1}{2}\Delta V^*_t + \frac{1}{2}\Delta V^*_d$$

$$\Delta V^*_p - \frac{1}{2}\Delta V^*_t = \Delta V^*_{poly} - \frac{1}{2}\Delta V^*_d \qquad (13)$$

Table 5 shows the values obtained for $k_p/k_t^{0.5}$ and k_d from the experimental data for copolymerization of VF2 with HFP and $k_p/k_t^{0.5}$ for PVDF homopolymerization. There is a good agreement between the estimated k_d for PBP in $scCO_2$ and the one reported for PBP decomposition in Freon 113 ($3.26 \times 10^{-4}\ s^{-1}$).[43] The value of $k_p/k_t^{0.5}$ for the copolymer is about half of that for PVDF. A low value of k_p is consistent with the much

Table 6. Reactivity Ratio Pairs for the Copolymerization of VF2 with HFP in the Literature

set no.	r_{HFP}	r_{VF2}	reference
A[a,d]	0	6.7	Moggi et al.[53]
B[a,d]	0	5	Logothetis et al.[30]
C[a,e]	0	2.45	Bonardelli et al.[54]
D[a,f]	0.12 ± 0.05	2.9 ± 0.6	Gelin et al.[52]
E[a,g]	0	5.13 ± 0.44	Tai et al.[42]
F[h]	0[a]	3.6[a]	Beginn et al.[41]
	0[b]	8.2[b]	
	0[c]	4.8[c]	
G[i]	0 ± 0.08[c]	3.61 ± 0.71[c]	Ahmed et al.[40]
	0.09 ± 0.09[c]	4.67 ± 0.77[c]	

[a] Based on copolymer composition obtained from NMR. [b] Based on copolymer composition obtained from F-EA. [c] Based on copolymer composition obtained from the average of both NMR and F-EA. [d] Batch emulsion polymerization at 70−130 °C and 20−70 bar (exact conditions not known). [e] Batch emulsion polymerization at 85 °C and 13.2 bar; values from NMR. [f] Batch solution polymerization in acetonitrile at 120 °C. [g] Batch precipitation polymerization in $scCO_2$ at 55 °C and initial pressure of 276 bar. [h] Batch polymerization in $scCO_2$ at 50 °C and initial pressure of 280 bar. [i] Batch polymerization in $scCO_2$ at 35 °C and initial pressure of 310 and 415 bar.

lower reactivity of the polymeric radicals with terminal HFP units compared to the radicals with terminal VF2 units. In fact, the reactivity ratio for HFP is essentially zero.[22−24,40] Consequently, HFP monomer units cannot add to growing chains with a terminal HFP unit. For the same reasons, the chemical kinetic termination rate constant is expected to be lower for the copolymerization than for the homopolymerization. However, since termination is diffusion-controlled, at least for the high-molecular-weight chains, the effect is weaker in the observed termination rate constant. In addition, $k_p/k_t^{0.5}$ is more sensitive to changes in k_p than in k_t.

Reactivity Ratios. Previously reported reactivity ratios for the copolymerization of VF2 with HFP are shown in Table 6. Although various investigators agree that the reactivity ratio of HFP is essentially zero, there are substantial differences in the value for VF2. This is probably due to differences from study to study in the mode of polymerization (emulsion, precipitation, solution, etc.), reaction conditions, and/or monomer composition drift for batch reactors. Additional differences can arise from the different analytical methods used for determining the copolymer composition. Most of the reported values are for copolymer compositions determined from NMR, and only few are from F-EA. Moreover, because of the heterogeneity of the polymerization systems, most of the reported values contain a "concentration factor" that changes with reaction conditions. Therefore, the reported values should be considered as "effective" reactivity ratios. The only exception is the reactivity ratios reported for solution polymerization in acetonitrile by Gelin et al. at 120 °C.[52]

For a CSTR, there is no composition drift. Consequently, the reactivity ratios calculated should be more accurate than those obtained from batch reactor experiments. Equation 14 is the differential form of the Mayo−Lewis equation.[55] On the basis of the data in Table 6, r_{HFP} was set equal to zero. For this case, eq 14 simplifies to eq 15, so that r_{VF2} can be calculated from the values of F_{HFP} and f_{HFP} (mole fraction of HFP in the effluent monomers, eq 16).

$$F_{HFP} = \frac{r_{HFP} f_{HFP}^{\ 2} + f_{HFP}(1 - f_{HFP})}{r_{HFP} f_{HFP}^{\ 2} + 2 f_{HFP}(1 - f_{HFP}) + r_{VF2}(1 - f_{HFP})^2} \quad (14)$$

$$r_{VF2} = \frac{\left(2 - \frac{1}{F_{HFP}}\right)}{\left(1 - \frac{1}{f_{HFP}}\right)} \quad (15)$$

$$f_{HFP} = \frac{(f_{HFP})_{in}[M_T]_{in} - \tau F_{HFP}(R_p)_{av}}{[M_T]_{out-av}} \quad (16)$$

where $(f_{HFP})_{in}$ is the mole fraction of HFP in the feed monomers to the reactor and F_{HFP} is the mole fraction of HFP in the copolymer, based on the average from NMR and F-EA.

Using the values of experiment 1 from Table 1, the "effective" reactivity ratio for VF2 for the copolymerization of VF2 with HFP in $scCO_2$ is

$$r_{VF2} = 3.2 \qquad \text{at 40 °C and 400 bar}$$

This value is very close to the value of 2.9 obtained from solution polymerization in acetonitrile by Gelin et al.[52] However, Gelin et al.'s experiments were at much higher temperature (120 °C) and in a batch reactor with about 10−12% VF2 conversion.[52]

Locus of Polymerization. The question of where the polymerization takes place is of both theoretical interest and practical importance. When polymer precipitates during the polymerization reaction, the reaction can take place either in the supercritical fluid phase, in the precipitated polymer particles, or simultaneously in both phases. For the precipitation copolymerization of VF2 with HFP, many features of the current results suggest that the copolymerization takes place mainly in the CO_2-rich fluid phase. First, the first-order dependence of both R_p and M_n on total monomer concentration, as shown in Figure 5a,b, is characteristic of a conventional solution polymerization. If the polymer phase was a significant polymerization locus, a higher order of dependence of both R_p and M_n on total monomer concentration should have been observed.[38] Second, the significant increase of both R_p and M_n with increasing pressure is consistent with the hypothesis that polymerization occurs primarily in the fluid phase. Besides the effect of pressure on the reaction rate constants discussed before, the increase in the pressure increases the solubility of the copolymer in $scCO_2$ and causes the growing chains to precipitate at higher molecular weights, leading to an increase in the concentration of polymer radicals in the fluid phase. This leads directly to an increase in R_p and M_n. Finally, the increased concentration of high molecular weight polymer radicals leads to the increase of the MWD tail with increasing pressure, since the effective termination rate constant decreases with increasing radical chain length.[50,56]

The bimodal MWD observed experimentally for the homopolymerization of VF2 in $scCO_2$[37,57] is the subject of some controversy. The bimodality has been attributed either to a simultaneous polymerization in both the fluid and the polymer phases, taking into account the transport of polymeric radicals between the two phases,[57] or to a homogeneous polymerization, recognizing the transition of the termination reaction from a kinetically controlled regime to a diffusion-controlled regime with increasing macroradical molecular weight.[56] For VF2/HFP copolymerization, the heterogeneous model cannot account for the increase of the tail with increasing pressure since transport of the polymeric radicals from the fluid phase to the polymer phase should decrease with increasing pressure as their diffusion coefficients decrease with pressure. On the other hand, according to the homogeneous model, the decrease of the diffusion

coefficient of the polymeric radicals with pressure leads to a lower effective termination rate constant, leading to the increase of the tail.

Finally, the slight decrease in HFP incorporation in the copolymer with increasing copolymer volume fraction may be the result of preferential partitioning of HFP into the precipitated copolymer particles. This could lead to a decrease of the HFP/VF2 ratio in the fluid phase, giving rise to lower HFP content copolymers. This explanation rationalizes the use of experiment 1 for calculating the reactivity ratio for VF2.

Conclusions

The continuous precipitation copolymerization of VF2 with HFP in $scCO_2$ was successfully carried out using PBP initiator in a CSTR. The copolymer was collected continuously as a dry, free-flowing powder. The effects of total monomer concentration and reaction pressure were both explored at otherwise constant conditions.

Both R_p and M_n increased linearly with total monomer concentration, and both increased with pressure by about 80% from 207 to 400 bar. This increase cannot be accounted for only by the effect of pressure on the reaction rate constants. The MWDs of the synthesized copolymer showed a long tail that became a broad shoulder with increasing total monomer concentration. This tail increased with increasing reaction pressure.

The $k_p/k_t^{0.5}$ ratio for the copolymerization is less than that for the homopolymerization of VF2 in $scCO_2$ at identical conditions. This was attributed to the low reactivity of HFP-terminated polymer radicals. The reactivity ratio of VF2 calculated from the experimental data is similar to the value reported for the solution polymerization of VF2 with HFP in acetonitrile.

Finally, the experimental data suggest that the CO_2-rich fluid phase is the primary locus of polymerization. Homogeneous polymerization in the CO_2-rich fluid phase can account for the first-order dependence of R_p and M_n on the total monomer concentration, the increase of R_p and M_n with pressure, and the increase of the MWD tail with pressure.

Acknowledgment. This material is based upon work supported by the STC Program of the National Science Foundation under Agreement No. CHE-9876674.

References and Notes

(1) Beckman, E. J. *J. Supercrit. Fluids* **2004**, *28* (2−3), 121−191.
(2) Canelas, D. A.; DeSimone, J. M. *Adv. Polym. Sci.* **1997**, *133*, 103−140.
(3) DeSimone, J. M. *Science* **2002**, *297* (5582), 799−803.
(4) Kendall, J. L.; Canelas, D. A.; Young, J. L.; DeSimone, J. M. *Chem. Rev.* **1999**, *99* (2), 543−563.
(5) Cooper, A. I. *J. Mater. Chem.* **2000**, *10* (2), 207−234.
(6) Kennedy, K. A.; Roberts, G. W.; DeSimone, J. M. *Adv. Polym. Sci.* **2005**, *175*, 329−346.
(7) Guan, Z.; Combes, J. R.; Menceloglu, Y. Z.; DeSimone, J. M. *Macromolecules* **1993**, *26* (11), 2663−9.
(8) Bunyard, W. C.; Kadla, J. F.; DeSimone, J. M. *J. Am. Chem. Soc.* **2001**, *123* (30), 7199−7206.
(9) Charpentier, P. A.; DeSimone, J. M.; Roberts, G. W. *Chem. Eng. Sci.* **2000**, *55* (22), 5341−5349.
(10) Liu, T.; Garner, P.; DeSimone, J. M.; Roberts, G. W.; Bothun, G. D. *Macromolecules* **2006**, *39* (19), 6489−6494.
(11) Saraf, M. K.; Wojcinski, L. M.; II.; Kennedy, K. A.; Gerard, S.; Charpentier, P. A.; DeSimone, J. M.; Roberts, G. W. *Macromol. Symp.* **2002**, *182*, 119−129.
(12) *Preliminary Risk Assessment: Perfluorooctanic Acid (PFOA) and Fluorinated Telomers*; US Environmental Protection Agency: April 2003.
(13) *2010/15 PFOA Stewardship Program*; U.S. Environmental Protection Agency: Jan 2006.
(14) McCoy, M. *Chem. Eng. News* **1999**, *77* (10).
(15) Press Release: DuPont introduces fluoropolymers made with supercritical CO_2 technology. DuPont, Wilmington, DE, 2002.
(16) Robinson, D.; Seiler, D. A. Modifications of PVDF resins leading to new fabrication opportunities with improved service life. In *Managing Corrosion with Plastics NACE Proceedings*, 1991; Vol. 10 (22), pp 1−14.
(17) Scheirs, J. *Modern Fluoropolymers: High Performance Polymers for Diverse Applications;* John Wiley & Sons: New York, 1997.
(18) Ameduri, B.; Boutevin, B.; Kostov, G. *Prog. Polym. Sci.* **2001**, *26* (1), 105−187.
(19) Solvay-Solexis, Solef & Hylar PVDF: Design and Processing Guide In www.Solvaysolexis.com/static/wma/pdf/9/2/2/3/br_Solef_Hylar.pdf.
(20) Apostolo, M.; Arcella, V.; Storti, G.; Morbidelli, M. *Macromolecules* **1999**, *32* (4), 989−1003.
(21) Ajroldi, G.; Pianca, M.; Fumagalli, M.; Moggi, G. *Polymer* **1989**, *30* (12), 2180−2187.
(22) Ferguson, R. C. *J. Am. Chem. Soc.* **1960**, *82* (10), 2416−2418.
(23) Pianca, M.; Bonardelli, P.; Tato, M.; Cirillo, G.; Moggi, G. *Polymer* **1987**, *28* (2), 224−230.
(24) Schmiegel, W. W. *Angew. Makromol. Chem.* 1979, *76−7* (Mar), 39−65.
(25) Kaspar, H. 3M Company, personal communication, 2003.
(26) Office for Official Publications of the European Communities. Document no.: 302M2690-Solvay/Montedison-Ausimont Merger Procedure (302M2690).
(27) Abusleme, J. A.; Gavezotti, P. Suspension (co)polymerization with bis(dichlorofluoroacetyl) peroxide for preparation of hydrogen-containing thermoplastic fluoropolymers. US Patent 5,569,728, 1995.
(28) Arnold, R. G.; Barney, A. L.; Thompson, D. C. *Rubber Chem. Technol.* **1973**, *46* (3), 619−52.
(29) Dixon, S.; Rexford, D. R.; Rugg, J. S. *Ind. Eng. Chem.* **1957**, *49* (10), 1687−1690.
(30) Logothetis, A. L. *Prog. Polym. Sci.* **1989**, *14* (2), 251−296.
(31) Stevens, M. P. *Polymer Chemistry: An Introduction*, 3rd ed.; Oxford University Press: New York, 1999.
(32) Howe-Grant, M. *Fluorine Chemistry: A Comprehensive Treatment;* Wiley: New York, 1995.
(33) Bonardelli, P.; Moggi, G.; Russo, S. *Makromol. Chem., Suppl.* **1985**, *10−11*, 11−23.
(34) Humphrey, J. S.; Amin-Sanayei, R. Vinylidene Fluoride Polymers. In *Encyclopedia of Polymer Science and Technology*, 3rd ed.; Mark, H. F., Ed.; Wiley: New York, 2004; Vol. 4, pp 510−533.
(35) Charpentier, P. A.; Kennedy, K. A.; DeSimone, J. M.; Roberts, G. W. *Macromol. Commun.* **1999**, *32* (18), 5973−5975.
(36) Charpentier, P. A.; DeSimone, J. M.; Roberts, G. W. *Ind. Eng. Chem. Res.* **2000**, *39* (12), 4588−4596.
(37) Saraf, M. K.; Gerard, S.; Wojcinski, L. M.; Charpentier, P. A.; DeSimone, J. M.; Roberts, G. W. *Macromolecules* **2002**, *35* (21), 7976−7985.
(38) Liu, T.; Desimone, J. M.; Roberts, G. W. *J. Polym. Sci., Part A: Polym. Chem.* **2005**, *43* (12), 2546−2555.
(39) Liu, T.; DeSimone, J. M.; Roberts, G. W. *Chem. Eng. Sci.* **2006**, *61* (10), 3129−3139.
(40) Ahmed, T. S.; DeSimone, J. M.; Roberts, G. W. *Macromolecules* **2006**, *39* (1), 15−18.
(41) Beginn, U.; Najjar, R.; Ellmann, J.; Vinokur, R.; Martin, R.; Moeller, M. *J. Polym. Sci., Part A: Polym. Chem.* **2006**, *44* (3), 1299−1316.
(42) Tai, H.; Wang, W.; Howdle, S. M. *Macromolecules* **2005**, *38* (22), 9135−9142.
(43) Zhao, C. X.; Zhou, R. M.; Pan, H. Q.; Jin, X. S.; Qu, Y. L.; Wu, C. J.; Jiang, X. K. *J. Org. Chem.* **1982**, *47* (11), 2009−2013.
(44) Reid, R. C.; Prausnitz, J. M.; Poling, B. E. *The Properties of Gases and Liquids*, 4th ed.; McGraw Hill: New York, 1987.
(45) Thomson, G. H.; Brobst, K. R.; Hankinson, R. W. *AIChE J.* **1982**, *28* (4), 671−676.
(46) Isbester, P. K.; Brandt, J. L.; Kestner, T. A.; Munson, E. J. *Macromolecules* **1998**, *31* (23), 8192−8200.
(47) Odian, G. *Principles of Polymerization*, 4th ed.; John Wiley & Sons: New York, 2004.
(48) Dohany, J. E. Poly(Vinylidene Fluoride). In *Kirk-Othmer Encyclopedia of Chemical Technology*, 4th ed.; Kirk-Othmer, Ed.; John Wiley & Sons: New York, 1998.
(49) Luft, G.; Ogo, Y. Activation Volumes of Polymerization Reactions. In *Polymer Handbook*, 4th ed.; Brandrup, J., Immergut, E. H., Grulke, E. A., Eds.; John Wiley & Sons: New York, 1999; p II-429.
(50) Matyjaszewski, K.; Davis, T. P. *Handbook of Radical Polymerization;* Wiley-Interscience: New York, 2002.
(51) Ito, K.; O'Driscoll, K. F. *J. Polym. Sci., Polym. Chem. Ed.* **1979**, *17*, (12), 3913−3921.

(52) Gelin, M.-P.; Ameduri, B. *J. Fluorine Chem.* **2005**, *126* (4), 577−585.
(53) Moggi, G.; Bonardelli, P.; Russo, S. *6th Conv. Ital. Sci. Macromol., [Atti]* **1983**, *2*, 405−408.
(54) Bonardelli, P.; Moggi, G.; Turturro, A. *Polymer* **1986**, *27* (6), 905−909.
(55) Mayo, F. R.; Lewis, F. M. *J. Am. Chem. Soc.* **1944**, *66* (9), 1594−1601.
(56) Ahmed, T. S.; DeSimone, J. M.; Roberts, G. W. *Chem. Eng. Sci.* **2004**, *59* (22−23), 5139−5144.
(57) Mueller, P. A.; Storti, G.; Apostolo, M.; Martin, R.; Morbidelli, M. *Macromolecules* **2005**, *38* (16), 7150−7163.

MA0713613